Outage Performance of Cognitive Hybrid Satellite Terrestrial Networks with Interference Constraint

Kang An[1], Min Lin[2,3], *Member, IEEE,* Wei-Ping Zhu[4] *Senior Member, IEEE*, Yongming Huang[5] *Member, IEEE* and Gan Zheng[6], *Senior Member, IEEE*

1. College of Communications Engineering, PLA University of Science and Technology, Nanjing, China

2. PLA University of Science and Technology, Nanjing, China

3. National Mobile Communications Research Laboratory, Southeast University, Nanjing, China

4. Department of Electrical and Computer Engineering, Concordia University, Montreal, Canada

5. School of Information Science and Engineering, Southeast University, Nanjing, China

6. School of Computer Science and Electronic Engineering, University of Essex, UK

(Emails: ankang@nuaa.edu.cn, linmin63@163.com, weiping@ece.concordia.ca, huangym@seu.edu.cn, ganzheng@essex.ac.uk)

Abstract

This paper investigates the performance of a cognitive hybrid satellite terrestrial network, where the primary satellite communication network and the secondary terrestrial mobile network coexist provided that the interference temperature constraint is satisfied. By using the Meijer-G functions, the exact closed-form expression of the outage probability (OP) for the secondary network is first derived. Then, the asymptotic result in high signal-to-noise ratio (SNR) regime is presented to reveal the diversity order and coding gain of the cognitive system. Finally, computer simulations are carried out to validate the theoretical results, indicating that a looser interference temperature constraint or a worse shadowing severity of satellite interfering link would lead to an improved outage performance, while a stronger satellite interference power poses a detrimental effect on the system performance.

Index Terms

Satellite terrestrial network, cognitive radio, outage performance, asymptotic result.

I. Introduction

Satellite communication has been widely used in various areas, such as broadcasting, disaster relief and navigation due to its potential in providing wide coverage and achieving higher data transmission rate at a low cost (see e.g., [1]-[3] and the references therein). Under this situation, many researches have investigated the key performance merits of satellite communications, such as outage probability (OP), average symbol error rate (ASER) and ergodic capacity [4]-[8]. However, the increasingly growing number of applications and services of satellite communication is rapidly exhausting the limited spectral resources, and therefore exploring new techniques to enhance spectrum efficiency in satellite communication has become an important research issue.

Cognitive radio (CR) is regarded as an effective means in the future mobile communications to increase the spectral efficiency, as it allows the secondary user (SU) to coexist with the primary user (PU), provided that the interference caused by the SU to each PU is properly regulated [9]-[11]. Inspired by the superiority of cognitive radio, several standardization groups (e.g. ETSI) and researchers have focused on the integration of the CR technology into satellite networks [12]-[14]. This idea constitutes a promising architecture, referred as cognitive hybrid satellite

terrestrial network , which allows the coexistence of a satellite network with a terrestrial one operating in the same frequency band.

To the best knowledge of the authors, only the recent work in [15] has investigated the capacity of a cognitive satellite terrestrial network based on the optimal power allocation scheme. However, no results of other important performance merits, such as outage probability, have been reported, which motivates the work presented in this paper. Here, we investigate the outage performance of cognitive satellite terrestrial network with interference constraint. Our main contribution is that by using the Meijer-G functions, a novel closed-form expression of outage probability for the considered cognitive network is derived. Furthermore, the asymptotic results at high SNR are also presented for both the proportional interference constraint as well as the peak interference constraint.

Notations: $\mathrm{E}[\cdot]$ denotes the expectation operator, $|\cdot|$ the absolute value, $\min(a,b)$ the minimum value of a and b, $\exp(\cdot)$ the exponential function, $\mathcal{N}_C(m,\sigma^2)$ the complex Gaussian distribution with mean m and variance σ^2.

II. Problem Formulation

As depicted in Fig. 1, we consider a cognitive hybrid satellite terrestrial network, where the terrestrial mobile network, acted as the secondary system, share the same spectral resource with the satellite communication network, termed as primary system, to improve the efficiency of the radio spectrum. Assuming that all of the nodes are equipped with a single antenna, the received signal of the terrestrial user, namely, SU, can be expressed as

$$y_d(t) = \sqrt{P_s} h_{ss} x(t) + \sqrt{P_p} g_{ps} s(t) + n(t) \tag{1}$$

where P_s and P_p denote, respectively, the transmit power at the base station (BS) and that at the satellite with $x(t)$ and $s(t)$ being the corresponding signals obeying $\mathrm{E}\left[|x(t)|^2\right] = 1$ and $\mathrm{E}\left[|s(t)|^2\right] = 1$. In addition, h_{ss} is the channel coefficient from base station to the secondary user, and g_{ps} is the channel coefficient of the interfering link from the satellite to secondary user. Meanwhile, $n(t) \sim \mathcal{N}_C\left(0,\sigma^2\right)$ represents the zero mean additive white Gaussian noise (AWGN) at SU.

To prevent the PU from being interfered beyond an interference temperature constraint Q, the transmit power at BS should satisfy [15]

$$P_s = \min\left(\frac{Q}{|h_{sp}|^2}, P_t\right) \tag{2}$$

where P_t denotes the maximum available transmit power at the BS, and g_{sp} is the channel coefficient between the base station and the primary user. Therefore, after some algebraic manipulations, the end-to-end signal-to-interference-plus-noise ratio (SINR) at SU can be written as

$$\gamma_d = \frac{P_s |h_{ss}|^2}{P_p |g_{ps}|^2 + \sigma^2} = \frac{\bar{\gamma}_s |h_{ss}|^2}{\bar{\gamma}_p |g_{ps}|^2 + 1} \tag{3}$$

where $\bar{\gamma}_s = P_s/\sigma^2$ and $\bar{\gamma}_p = P_p/\sigma^2$ denote the average signal-to-noise ratio (SNR).

Satellite links are usually modeled by composite fading distributions to describe more accurately the amplitude fluctuation of the signal envelope. Although some mathematical models, such as Loo, Barts-Stutzman, and Karasawa *et al.*, have been presented to describe the satellite channel, the Shadowed-Rician model proposed in [16] is a popular

one, which provides a significantly less computational burden than other channel models. The fading channel of the satellite links can be modeled as $g_k = \bar{g}_k + j\tilde{g}_k, j^2 = -1 \left(k \triangleq pp, ps\right)$, where the line-of-sight (LoS) component $\bar{g}_k$ can be described as an independent and identically distributed (i.i.d) Nakagami-m random variable (RV), and the element of scattering component $\tilde{g}_k$ follows an i.i.d complex Gaussian distribution with zero mean. Consequently, the probability density function (PDF) of $Y_k = |g_k|^2 \left(k \triangleq pp, ps\right)$ is given by [4]-[7], [16]

$$f_{Y_k}(x) = \alpha_k \exp(-\beta_k x)\, {}_1F_1(m_k; 1; \delta_k x) \tag{4}$$

where ${}_1F_1(a; b; c)$ represents the confluent hypergeometric function [17, eq. (9.210.1)], $\alpha_k = 2b_k m_k/(2b_k m_k + \Omega_k)^{m_k}/2b_k$, $\beta_k = 1/2b_k$, $\delta_k = \Omega_k/2b_k(2b_k m_k + \Omega_k)$ with Ω_k being the average power of LOS component, $2b_k$ the average power of the multipath component, and m_k the Nakagami-m parameter ranging from 0 to ∞.

Similar to [5]-[6], we consider that the terrestrial links, namely h_{ss} and h_{sp}, undergo Nakagami-m fading distribution. Thus, $X_i = |h_i|^2 \left(i \triangleq ss, sp\right)$ is subject to the Gamma distribution, whose PDF is given by [15]

$$f_{X_i}(x) = \frac{\varepsilon_i^{m_i} x^{m_i - 1}}{\Gamma(m_i)} \exp(-\varepsilon_i x) \tag{5}$$

where $\Gamma(\cdot)$ is the Gamma function [17, eq. (8.310.1)], and $\varepsilon_i = m_i/\Omega_i$ with m_i and Ω_i being the fading severity parameter and the average power, respectively.

In the following sections, based on the above-mentioned statistical properties of the fading links, we will analyze the OP of the secondary network by deriving some useful expressions.

III. Outage Probability Analysis

In wireless systems, the outage probability is an important quality-of-service (QoS) performance measure, which is defined as the probability that the output instantaneous SINR γ_d falls below an acceptable threshold γ_{th}, namely,

$$P_{out}(\gamma_d \le \gamma_{th}) = F_{\gamma_d}(\gamma_{th}) \tag{6}$$

where $F_{\gamma_d}(x)$ denotes the cumulative distributed function (CDF). With the help of (3), $F_{\gamma_d}(x)$ can be written as

$$F_{\gamma_d}(x) = \Pr\left(\frac{\bar{\gamma}_s X_{ss}}{\bar{\gamma}_p Y_{ps} + 1} \le x\right) = \int_0^\infty F_{\bar{\gamma}_s X_{ss}}\left[x(\bar{\gamma}_p y + 1)\right] f_{Y_{ps}}(y)\, dy \tag{7}$$

To obtain (7), we first need to calculate $F_{\bar{\gamma}_s X_{ss}}(x)$. Based on (1), we have

$$\bar{\gamma}_s X_{ss} = \frac{P_s}{\sigma^2} X_{ss} = \min\left(\frac{Q}{|h_{sp}|^2 \sigma^2}, \frac{P_t}{\sigma^2}\right) X_{ss} = \min\left(\frac{\bar{\gamma}_Q}{|h_{sp}|^2}, \bar{\gamma}_t\right) X_{ss} \tag{8}$$

where $\bar{\gamma}_Q = Q/\sigma^2, \bar{\gamma}_t = P_t/\sigma^2$. As for any random variables A and B, of course we have min(A,B)=A if $B \ge A$ and min(A,B)=A if $B \le A$. Therefore, the CDF of $\bar{\gamma}_s X_{ss}$ can be expressed as the sum of the following probabilities,

$$F_{\bar{\gamma}_s X_{ss}}(x) = \Pr\left(\bar{\gamma}_t X_{ss} \le x, \bar{\gamma}_t \le \frac{\bar{\gamma}_Q}{|h_{sp}|^2}\right) + \Pr\left(\frac{\bar{\gamma}_Q}{|h_{sp}|^2} X_{ss} \le x, \bar{\gamma}_t > \frac{\bar{\gamma}_Q}{|h_{sp}|^2}\right) \tag{9}$$

Then, invoking again the concepts of conditional probability theory [18], $F_{\bar{\gamma}_s X_{ss}}(x)$ can be further expressed as

$$F_{\bar{\gamma}_s X_{ss}}(x) = \underbrace{\int_0^{\bar{\gamma}_Q/\bar{\gamma}_t} F_{X_{ss}}\left(\frac{x}{\bar{\gamma}_t}\right) f_{X_{sp}}(y)\, dy}_{I_1} + \underbrace{\int_{\bar{\gamma}_Q/\bar{\gamma}_t}^{\infty} F_{X_{ss}}\left(\frac{xy}{\bar{\gamma}_Q}\right) f_{X_{sp}}(y)\, dy}_{I_2} \tag{10}$$

where $F_{X_{ss}}(x)$ is the CDF of X_{ss}, which can be obtained by using [17, eq. (3.351.1)] as

$$F_{X_{ss}}(x) = \frac{\gamma(m_{ss}, \varepsilon_{ss} x)}{\Gamma(m_{ss})} = 1 - \exp(-\varepsilon_{ss} x) \sum_{k=0}^{m_{ss}-1} \frac{(\varepsilon_{ss} x)^k}{\Gamma(k+1)} \tag{11}$$

where $\gamma(\cdot,\cdot)$ is the lower incomplete Gamma function [17, eq. (8.350.1)].Then, by using (5) and (11) along wiht some algebraic computations, I_1 and I_2 in (10) can be computed as

$$I_1 = \exp\left(-\frac{\varepsilon_{ss} x}{\bar{\gamma}_t}\right) \sum_{k=0}^{m_{ss}-1} \frac{1}{\Gamma(k+1)} \left(\frac{\varepsilon_{ss} x}{\bar{\gamma}_t}\right)^k \frac{\gamma\left(m_{sp}, \varepsilon_{sp}\bar{\gamma}_Q/\bar{\gamma}_t\right)}{\Gamma(m_{sp})} \tag{12}$$

$$I_2 = \sum_{k=0}^{m_{ss}-1} \frac{1}{\Gamma(k+1)} \left(\frac{\varepsilon_{ss} x}{\bar{\gamma}_Q}\right)^k \frac{\varepsilon_{sp}^{m_{sp}}}{\Gamma(m_{sp})} \exp\left(-\frac{\bar{\gamma}_Q}{\bar{\gamma}_t}\left(\frac{\varepsilon_{ss} x}{\bar{\gamma}_Q} + \varepsilon_{sp}\right)\right) \sum_{n=0}^{k+m_{sp}-1} \frac{\Gamma(k+m_{sp})}{\Gamma(n+1)} \left(\frac{\bar{\gamma}_Q}{\bar{\gamma}_t}\right)^n \left(\frac{\varepsilon_{ss} x}{\bar{\gamma}_Q} + \varepsilon_{sp}\right)^{-(k+m_{sp}-n)} \tag{13}$$

In deriving (12) and (13), we have used the identity [17, eq. (3.351.1)] and [17, eq. (3.351.2)], respectively. Consequently, by substituting (12) and (13) into (10), one can obtain the analytical expression of $F_{\bar{\gamma}_s X_{ss}}(x)$ as

$$\begin{aligned} F_{\bar{\gamma}_s X_{ss}}(x) = 1 - \exp\left(-\frac{\varepsilon_{ss} x}{\bar{\gamma}_t}\right) \sum_{k=0}^{m_{ss}-1} \frac{1}{\Gamma(k+1)} \left(\frac{\varepsilon_{ss} x}{\bar{\gamma}_t}\right)^k \Bigg[\frac{\gamma\left(m_{sp}, \varepsilon_{sp}\bar{\gamma}_Q/\bar{\gamma}_t\right)}{\Gamma(m_{sp})} \\ + \frac{\varepsilon_{sp}^{m_{sp}}}{\Gamma(m_{sp})} \exp\left(-\frac{\varepsilon_{sp}\bar{\gamma}_Q}{\bar{\gamma}_t}\right) \sum_{n=0}^{k+m_{sp}-1} \frac{\Gamma(k+m_{sp})}{\Gamma(n+1)} \left(\frac{\bar{\gamma}_Q}{\bar{\gamma}_t}\right)^n \left(\frac{\varepsilon_{ss} x}{\bar{\gamma}_Q} + \varepsilon_{sp}\right)^{-(k+m_{sp}-n)} \Bigg] \end{aligned} \tag{14}$$

Finally, by substituting (14) into (7), F_{γ_d} can be calculated as shown in the following theorem.

Theorem 1. *The closed-form expression of $F_{\gamma_d}(x)$ can be computed as*

$$\begin{aligned} F_{\gamma_d}(x) = 1 - \frac{\alpha_{ps}}{\Gamma(m_{ps})\Gamma(m_{sp})} \exp\left(-\frac{\varepsilon_{ss} x}{\bar{\gamma}_t}\right) \sum_{k=0}^{m_{ss}-1} \frac{1}{\Gamma(k+1)} \left(\frac{\varepsilon_{ss} x}{\bar{\gamma}_t}\right)^k \sum_{q=0}^{k} \binom{k}{q} \frac{\bar{\gamma}_I^q}{\xi^{q+1}} \\ \times \left[\gamma\left(m_{sp}, \frac{\varepsilon_{sp}\bar{\gamma}_Q}{\bar{\gamma}_t}\right) \mathrm{G}_{2,2}^{1,2}\left[-\frac{\delta_{ps}}{\xi} \middle| \begin{matrix} -q, 1-m_{ps} \\ 0, 0 \end{matrix} \right] + \frac{\varepsilon_{sp}^{m_{sp}}}{\Gamma(m_{sp})} \exp\left(-\frac{\varepsilon_{sp}\bar{\gamma}_Q}{\bar{\gamma}_t}\right) \right. \\ \left. \times \sum_{n=0}^{k+m_{sp}-1} \frac{\Gamma(k+m_{sp})}{\Gamma(n+1)} \left(\frac{\bar{\gamma}_Q}{\bar{\gamma}_t}\right)^n \frac{\theta^{-(k+m_{sp}-n)}}{\Gamma(\eta)} \mathrm{G}_{1,[1:1],0,[1:2]}^{1,1,1,1,1} \left[\begin{matrix} \frac{\varepsilon_{ss} x}{\theta\xi\bar{\gamma}_Q} \\ -\frac{\delta_{ps}}{\xi} \end{matrix} \middle| \begin{matrix} q+1 \\ 1-\eta; 1-m_{ps} \\ -- \\ 0; 0, 0 \end{matrix} \right] \right] \end{aligned} \tag{15}$$

where $\xi = \varepsilon_{ss} x/\bar{\gamma}_t + \beta_{ps}$, $\eta = k + m_{sp} - n$ and $\theta = \varepsilon_{ss} x/\bar{\gamma}_Q + \varepsilon_{sp}$. In (16), $\mathrm{G}_{2,2}^{1,2}[\cdot|\cdot]$ is the Meijer-G function with single variable [17, eq. (9.301)], and $\mathrm{G}_{1,[1:1],0,[1:2]}^{1,1,1,1,1}[\cdot|\cdot]$ the Meijer-G function with two variables [19].

Proof. See Appendix A. □

Eventually, by replacing x with γ_{th} in (15), it is straightforward to calculate the OP of the considered cognitive network.

Remark 1. *Note that the Meijer-G function of single variable can be efficiently calculated by many popular computing softwares, such as Matlab and Mathematic, and the Meijer-G functions of two variables can be alternatively computed using an efficient approach proposed in [20, Table II]. As a conclusion, our theoretical formula provides an efficient method to evaluate the OP of the considered network with a low computational complexity.*

IV. Asymptotic Outage Probability at High SNR

In this section, we will study the asymptotic OP of the cognitive network and thereby reveal two important performance merits: diversity order and array gain. Herein, we consider two practical scenarios: A) proportional interference constraint, and B) peak interference constraint.

A. Proportional Interference Constraint

As for the proportional interference constraint scenario, the interference temperature constraint Q at PU is proportional to the maximum available transmit power $\bar{\gamma}_t$ at BS, i.e., $\bar{\gamma}_Q = \mu\bar{\gamma}_t$ with μ being the positive constant, which means that PU can tolerate a large power interference signal. In what follows, we will present the asymptotic outage probability of the secondary terrestrial network as Theorem 2.

Theorem 2. *The asymptotic OP at high SNR with proportional interference constraint can be expressed as*

$$P_{out}^{\infty}\left(\gamma_{th}\right) \approx \Upsilon \left(\frac{\gamma_{th}}{\bar{\gamma}_t}\right)^{m_{ss}} \tag{16}$$

where Υ *is given by*

$$\Upsilon = \left[\frac{\gamma\left(m_{sp}, \mu\varepsilon_{sp}\right)}{\Gamma\left(m_{sp}\right)\Gamma\left(m_{ss}+1\right)} + \frac{\Gamma\left(m_{ss}+m_{sp}, \mu\varepsilon_{sp}\right)}{\Gamma\left(m_{sp}\right)\Gamma\left(m_{ss}+1\right)\left(\mu\varepsilon_{sp}\right)^{m_{ss}}}\right] \times \frac{\alpha_{ps}\bar{\gamma}_p^k}{\Gamma\left(m_{ps}\right)\beta_{ps}^{k+1}} \sum_{k=0}^{m_{ss}} \binom{m_{ss}}{k} \mathrm{G}_{2,2}^{1,2}\left[-\delta_{ps} \middle| \begin{matrix} -k, 1-m_{ps} \\ 0, 0 \end{matrix}\right] \varepsilon_{ss}^{m_{ss}} \tag{17}$$

Proof. See Appendix B. □

According to the results reported in [22], we express the asymptotic OP expression in (16) into a general form with respective to the diversity order G_d and coding gain G_c, namely

$$P_{out}^{\infty}\left(\gamma_{th}\right) \approx \left(\frac{\Upsilon^{-m_{ss}^{-1}}}{\gamma_{th}}\bar{\gamma}_t\right)^{-m_{ss}} = \left(G_c\bar{\gamma}_t\right)^{-G_d} \tag{18}$$

Based on (18), one can directly observe the two performance metrics, namely, the diversity order G_d and coding gain G_c of the considered cognitive network, as $G_d = m_{ss}$ and $G_c = \Upsilon^{-m_{ss}^{-1}} \Big/ \gamma_{th}$.

B. Peak Interference Constraint

Besides the proportional interference constraint, we consider the peak interference constraint scenario, where Q is fixed and only P_t becomes large in the high SNR regime. The asymptotic behaviors of the secondary terrestrial network in this case is presented as Theorem 3 below.

Theorem 3. *The asymptotic OP in high SNR regime with peak interference constraint can be derived as*

$$P_{out}^{\infty}\left(\gamma_{th}\right) \approx \Theta\left(\frac{\gamma_{th}}{\bar{\gamma}_t}\right)^{m_{ss}} + \Xi\left(\frac{\gamma_{th}}{\bar{\gamma}_Q}\right)^{m_{ss}} \tag{19}$$

where

$$\Theta = \frac{\gamma\left(m_{sp}, \varepsilon_{sp}\bar{\gamma}_Q/\bar{\gamma}_t\right)\varepsilon_{ss}^{m_{ss}}}{\Gamma\left(m_{sp}\right)\Gamma\left(m_{ss}+1\right)} \frac{\alpha_{ps}\bar{\gamma}_p^k}{\Gamma\left(m_{ps}\right)\beta_{ps}^{k+1}} \sum_{k=0}^{m_{ss}} \binom{m_{ss}}{k} \mathrm{G}_{2,2}^{1,2}\left[-\delta_{ps} \middle| \begin{matrix} -k, 1-m_{ps} \\ 0, 0 \end{matrix}\right] \tag{20}$$

and

$$\Xi = \frac{\Gamma\left(m_{ss}+m_{sp}, \varepsilon_{sp}\bar{\gamma}_Q/\bar{\gamma}_t\right)}{\Gamma\left(m_{sp}\right)\Gamma\left(m_{ss}+1\right)} \left(\frac{\varepsilon_{ss}}{\varepsilon_{sp}}\right)^{m_{ss}} \frac{\alpha_{ps}\bar{\gamma}_p^k}{\Gamma\left(m_{ps}\right)\beta_{ps}^{k+1}} \sum_{k=0}^{m_{ss}} \binom{m_{ss}}{k} \mathrm{G}_{2,2}^{1,2}\left[-\delta_{ps} \middle| \begin{matrix} -k, 1-m_{ps} \\ 0, 0 \end{matrix}\right] \tag{21}$$

Proof. See Appendix C. □

For the peak interference constraint, it is worth noting that the OP performance becomes saturated in high SNR regime $\bar{\gamma}_t$, which means only zero diversity can be achieved. This is because the interference temperature constraint Q becomes a dominant factor to determine the maximum available transmit power at BS as shown in (2) in the case of $P_t \to \infty$.

V. Numerical Results

This section provides numerical results to show the validity of the theoretical analysis and the effects of key parameters on the system outage performance. Here, the simulation results are obtained by performing 10^7 channel realizations, the different shadowing scenarios of the satellite links (g_{ps}, g_{pp}), including frequent heavy shadowing (FHS), average shadowing (AS) and infrequent light shadowing (ILS), are given in Table I [16]. In the simulations, we set $\gamma_{th} = 3$ dB, $\Omega_{ss} = \Omega_{sp} = 1$ and the noise variance $\sigma^2 = 1$.

First of all, we focus on scenarios A), namely, proportional interference constraint. Fig. 2 plots the exact and asymptotic OP curves of the secondary terrestrial system for different satellite interference powers (i.e., P_p). As shown in the figure, the analytical results calculated by (15) agree well with the Monte Carlo simulation results, validating our theoretical derivations. Meanwhile, the outage performance significantly improves with the increase of m_{ss}, which reveals that the outage performance is closely related to the channel quality of the secondary transmission link h_{ss}. Moreover, the diversity order of m_{ss} can be achieved for the proportional interference constraint, which confirms our findings in the asymptotic analysis. Although the satellite interference power does not affect the system diversity order, it degrades the system performance by reducing the coding gain. Fig. 3 shows the impact of terrestrial interfering link quality (i.e. m_{ps}) on the OP of secondary network. Interestingly, the system performance with good terrestrial interfering link quality (i.e., large m_{sp}) is superior to that of bad terrestrial interfering link quality (i.e.,

small m_{sp}). This phenomenon reveals that the more deterministic the terrestrial interfering link is, the better outage performance can be achieved. Besides, it can also be observed that the outage performance improvement due to better interfering links becomes much more pronounced when the channel parameters of the SU link $(i.e., h_{ss})$ improves from 1 to 3, which indicates that the impact of terrestrial interfering link quality on the system performance is intimately related to the channel quality of the SU link.

Now, we consider scenario B), namely, peak interference constraint. The effect of different interference temperature constraints Q on the outage probability of secondary terrestrial network is shown in Fig. 4. Here, we consider $Q=-\infty, 10, 15, 20$dB, where the case of no interference temperature constraint denoted as $Q=-\infty$ is provided as a benchmark for comparison. As observed, the outage probability of the system under an interference temperature constraint is generally inferior to that of the system with no interference temperature constraint. Also, due to the existence of interference temperature constraint, the outage probability of the system becomes saturated, and the system diversity is reduced from m_{ss} to zero. Moreover, as the interference temperature constraint becomes loose, i.e., Q gets larger, the outage error floor reduces, and the outage performance of the system improves. Fig. 5 plots the impact of terrestrial interfering link quality (i.e. m_{ps}) on the outage performance of secondary network. Similar to scenario A), we can find that the impact of the terrestrial interfering link quality on the performance of secondary network heavily relies on the SU link.

Finally, Fig. 6 compares the outage performance of the secondary network for different shadowing severity of satellite interfering link (i.e. $(b_{ps}, m_{ps}, \Omega_{ps})$) between scenario A) and scenario B). As seen in the figure, for both scenarios, the comparison between FHS, AS and ILS curves shows that the cases experiencing heavier shadowing severity result in a worse outage performance. Moreover, it is found that the peak interference constraint is a litter better than the proportional interference constraint in low and medium SNR regimes. However, due to outage error floor where only zero diversity order can be achieved, the proportional interference constraint is significantly superior to the peak interference constraint at high SNR.

VI. Conclusions

In this paper, we have investigated the outage performance of a novel cognitive satellite-terrestrial network with interference temperature constraint, where the satellite system acts as the primary network while the terrestrial system serves as the secondary network. Both the exact and asymptotic expressions for the OP of the considered cognitive system have been derived in the closed-from, whose validity has been confirmed by Monte Carlo simulations. The proposed novel expression contains finite number of summation of generalized Meijer-G functions, which can evaluate the system performance with highly computational efficiency. Our finding shows that whether the fading severity of SU link affects the diversity order of the terrestrial cognitive system depends on the interference temperature constraint at PU. Particularly, under a peak interference constraint, the OP becomes saturated and no diversity order can be achieved. Furthermore, a worse shadowing severity of the satellite interfering link poses an detrimental impact on the performance of the cognitive network. Since the associated performance analysis of cognitive systems is a key research area in the practical wireless communication networks, our technical presentation

contributes to the engineers for the purpose of system design and performance evaluation.

APPENDIX A
PROOF OF THEOREM 1

By substituting $F_{\bar{\gamma}_s X_{ss}}(x)$ in (14) and $f_{X_{sp}}(x)$ in (5) into (7) along with binomial expansion, $F_{\gamma_d}(x)$ can be expressed as

$$F_{\gamma_d}(x) = 1 - \frac{\alpha_{ps}}{\Gamma(m_{sp})} \exp\left(-\frac{\varepsilon_{ss}x}{\bar{\gamma}_t}\right) \sum_{k=0}^{m_{ss}-1} \frac{1}{\Gamma(k+1)} \left(\frac{\varepsilon_{ss}x}{\bar{\gamma}_t}\right)^k \sum_{q=0}^{k} \binom{k}{q} \bar{\gamma}_p^q \left[\frac{\gamma\left(m_{sp}, \varepsilon_{sp}\bar{\gamma}_Q/\bar{\gamma}_t\right)}{\Gamma(m_{sp})}\right.$$
$$\times \underbrace{\int_0^\infty y^q \exp(-\xi y)\, {}_1F_1(m_{ps}; 1; \delta_{ps}y)\, dy}_{I_3} + \varepsilon_{sp}^{m_{sp}} \exp\left(-\frac{\varepsilon_{sp}\bar{\gamma}_Q}{\bar{\gamma}_t}\right) \sum_{n=0}^{k+m_{sp}-1} \frac{\Gamma(k+m_{sp})}{\Gamma(n+1)}$$
$$\left. \times \sum_{n=0}^{k+m_{sp}-1} \frac{\Gamma(k+m_{sp})}{\Gamma(n+1)} \left(\frac{\bar{\gamma}_Q}{\bar{\gamma}_t}\right)^n \underbrace{\int_0^\infty y^q \exp(-\xi y) \left(\frac{\varepsilon_{ss}xy}{\bar{\gamma}_Q} + \theta\right)^{-\eta} {}_1F_1(m_{ps}; 1; \delta_{ps}y)\, dy}_{I_4} \right] \quad (22)$$

where $\xi = \varepsilon_{ss}x/\bar{\gamma}_t + \beta_{ps}$, $\theta = \varepsilon_{ss}x/\bar{\gamma}_Q + \varepsilon_{sp}$ and $\eta{=}k + m_{sp} - n$. Since the integrals I_3 and I_4 in (22) can not be directly evaluated in their current form, we then proposed a Meijer-G function based mathematic methodology in the following derivation.

To compute I_3, we first apply [17, eq. (8.455.1)] and express the hypergeometric function ${}_1F_1(m_{ps}; 1; \delta_{ps}y)$ in terms of the Meijer-G functions as

$${}_1F_1(m_{ps}; 1; \delta_{ps}y) = \frac{1}{\Gamma(m_{ps})} \mathrm{G}_{1,2}^{1,1}\left[-\delta_{ps}y \,\middle|\, \begin{matrix} 1-m_{ps} \\ 0, 0 \end{matrix}\right] \quad (23)$$

Then, with the help of [17, eq. (7.813.1)], we obtain

$$I_3 = \frac{\xi^{-q-1}}{\Gamma(m_{ps})} \mathrm{G}_{2,2}^{1,2}\left[-\frac{\delta_{ps}}{\xi} \,\middle|\, \begin{matrix} -q, 1-m_{ps} \\ 0, 0 \end{matrix}\right] \quad (24)$$

where $\mathrm{G}_{2,2}^{1,2}[\cdot\,|\cdot]$ is the Meijer-G functions with single variable [17, eq. (9.301)]. As for I_4, according to [21, eq. (10), (11)], we express the functions $\exp(-\xi y)$ and $(\varepsilon_{ss}xy/\bar{\gamma}_Q + \theta)^{-\eta}$ in terms of Meijer-G function as

$$\exp(-\xi y) = \mathrm{G}_{01}^{1,0}\left[\xi y \,\middle|\, \begin{matrix} - \\ 0 \end{matrix}\right], \quad \left(\frac{\varepsilon_{ss}xy}{\bar{\gamma}_Q} + \theta\right)^{-\eta} = \frac{1}{\Gamma(\eta)\theta^\eta} \mathrm{G}_{1,1}^{1,1}\left[\frac{\varepsilon_{ss}xy}{\bar{\gamma}_Q\theta} \,\middle|\, \begin{matrix} 1-\eta \\ 0 \end{matrix}\right] \quad (25)$$

Then, by using (25) and (25), and applying [19, eq. (3.1)], we have

$$I_4 = \frac{\xi^{-(q+1)}}{\Gamma(m_{ps})\Gamma(\eta)\theta^\eta} \mathrm{G}_{1,[1:1],0,[1:2]}^{1,1,1,1,1}\left[\begin{matrix} \frac{\varepsilon_{ss}x}{\theta\xi\bar{\gamma}_Q} \\ -\frac{\delta_{ps}}{\xi} \end{matrix} \,\middle|\, \begin{matrix} q+1 \\ 1-\eta; 1-m_{ps} \\ -- \\ 0; 0, 0 \end{matrix}\right] \quad (26)$$

where $\mathrm{G}_{1,[1:1],0,[1:2]}^{1,1,1,1,1}[\cdot\,|\,\cdot]$ denotes the Meijer-G functions with two variables [19]. Substituting (24) and (26) into (22) and conducting some necessary computations, one can obtain (15).

APPENDIX B
PROOF OF THEOREM 2

By using (10) along with $\mu = \bar{\gamma}_Q/\bar{\gamma}_t$, $F^{\infty}_{\bar{\gamma}_s X_{ss}}(x)$ for the proportional interference constraint can be expressed as

$$F^{\infty}_{\bar{\gamma}_s X_{ss}}(x) = \underbrace{\int_0^{\mu} F^{\infty}_{X_{ss}}\left(\frac{x}{\bar{\gamma}_t}\right) f_{X_{sp}}(y)dy}_{\widehat{I}_1} + \underbrace{\int_{\mu}^{\infty} F^{\infty}_{X_{ss}}\left(\frac{x}{\mu\bar{\gamma}_t}y\right) f_{X_{sp}}(y)\,dy}_{\widehat{I}_2} \tag{27}$$

Hence, in order to obtain (27), we first need to obtain the asymptotic CDF of X_{ss}. Since the asymptotic results only depend on the high order terms [6], i.e., $\bar{\gamma}_t \to \infty$, we apply series representation of incomplete Gamma function [17, eq. (8.354.1)] as

$$\gamma(m_i, \varepsilon_i z) = (\varepsilon_i z)^{m_i} \sum_{n=0}^{\infty} \frac{(-1)^n (\varepsilon_i z)^n}{n!\,(m_i+n)} \overset{z\to 0}{\approx} \frac{(\varepsilon_i z)^{m_i}}{m_i} \tag{28}$$

to $F_{X_{ss}}(x)$ in (11), and obtain its asymptotic form as

$$F^{\infty}_{X_i}(x) \approx \frac{(\varepsilon_i x)^{m_i}}{\Gamma(m_i+1)} \tag{29}$$

By using (5) and (29) into (27), and applying [17, eq. (3.352.1), eq. (3.352.2)], we have

$$\widehat{I}_1 \approx \frac{1}{\Gamma(m_{ss}+1)}\left(\frac{\varepsilon_{ss}x}{\bar{\gamma}_t}\right)^{m_{ss}} \int_0^{\mu} \frac{\varepsilon_{sp}^{m_{sp}} y^{m_{sp}-1}}{\Gamma(m_{sp})} \exp(-\varepsilon_{sp}y)dy = \frac{\gamma(m_{sp}, \mu\varepsilon_{sp})}{\Gamma(m_{sp})\Gamma(m_{ss}+1)}\left(\frac{\varepsilon_{ss}x}{\bar{\gamma}_t}\right)^{m_{ss}} \tag{30}$$

$$\widehat{I}_2 \approx \frac{1}{\Gamma(m_{ss}+1)}\left(\frac{\varepsilon_{ss}x}{\mu\bar{\gamma}_t}\right)^{m_{ss}} \int_{\mu}^{\infty} \frac{\varepsilon_{sp}^{m_{sp}} y^{m_{ss}+m_{sp}-1}}{\Gamma(m_{sp})} \exp(-\varepsilon_{sp}y)\,dy = \frac{\Gamma(m_{ss}+m_{sp}, \mu\varepsilon_{sp})}{\Gamma(m_{sp})\Gamma(m_{ss}+1)}\left(\frac{\varepsilon_{ss}x}{\mu\varepsilon_{sp}\bar{\gamma}_t}\right)^{m_{ss}} \tag{31}$$

Then, substituting (30) and (31) into (27), and performing necessary manipulation yields

$$F^{\infty}_{\bar{\gamma}_s X_{ss}}(x) \approx \left[\frac{\gamma(m_{sp}, \mu\varepsilon_{sp})}{\Gamma(m_{sp})\Gamma(m_{ss}+1)} + \frac{\Gamma(m_{ss}+m_{sp}, \mu\varepsilon_{sp})}{\Gamma(m_{sp})\Gamma(m_{ss}+1)(\mu\varepsilon_{sp})^{m_{ss}}}\right]\left(\frac{\varepsilon_{ss}x}{\bar{\gamma}_t}\right)^{m_{ss}} \tag{32}$$

Using (6) and (32) into (7), and applying [17, eq. (7.813.1)], we have

$$\begin{aligned} F^{\infty}_{\gamma_d}(x) \approx & \left[\frac{\gamma(m_{sp}, \mu\varepsilon_{sp})}{\Gamma(m_{sp})\Gamma(m_{ss}+1)} + \frac{\Gamma(m_{ss}+m_{sp}, \mu\varepsilon_{sp})}{\Gamma(m_{sp})\Gamma(m_{ss}+1)(\mu\varepsilon_{sp})^{m_{ss}}}\right] \\ & \times \frac{\alpha_{ps}\bar{\gamma}_p^k}{\Gamma(m_{ps})\beta_{ps}^{k+1}} \sum_{k=0}^{m_{ss}} \binom{m_{ss}}{k} \mathrm{G}^{1,2}_{2,2}\left[-\delta_{ps}\middle|\begin{matrix}-k, 1-m_{ps}\\ 0, 0\end{matrix}\right]\left(\frac{\varepsilon_{ss}x}{\bar{\gamma}_t}\right)^{m_{ss}} \end{aligned} \tag{33}$$

Finally, by replacing x in (33) with γ_{th}, the asymptotic OP can be obtained as (16).

APPENDIX C
PROOF OF THEOREM 3

By using (10), the asymptotic CDF of $\bar{\gamma}_s X_{ss}$ for peak interference constraint can be obtained as

$$F^{\infty}_{\bar{\gamma}_s X_{ss}}(x) = \underbrace{\int_0^{\bar{\gamma}_Q/\bar{\gamma}_t} F^{\infty}_{X_{ss}}\left(\frac{x}{\bar{\gamma}_t}\right) f_{X_{sp}}(y)\,dy}_{\breve{I}_1} + \underbrace{\int_{\bar{\gamma}_Q/\bar{\gamma}_t}^{\infty} F^{\infty}_{X_{ss}}\left(\frac{xy}{\bar{\gamma}_Q}\right) f_{X_{sp}}(y)\,dy}_{\breve{I}_2} \tag{34}$$

Applying the similar approaches in obtaining (30) and (31), $\breve{I}_1$ and $\breve{I}_2$ can be, respectively, computed as

$$\breve{I}_1 = \frac{\gamma\left(m_{sp}, \varepsilon_{sp}\bar{\gamma}_Q/\bar{\gamma}_t\right)}{\Gamma\left(m_{sp}\right)\Gamma\left(m_{ss}+1\right)}\left(\frac{\varepsilon_{ss}x}{\bar{\gamma}_t}\right)^{m_{ss}}, \quad \breve{I}_2 = \frac{\Gamma\left(m_{ss}+m_{sp}, \varepsilon_{sp}\bar{\gamma}_Q/\bar{\gamma}_t\right)}{\Gamma\left(m_{sp}\right)\Gamma\left(m_{ss}+1\right)}\left(\frac{\varepsilon_{ss}x}{\varepsilon_{sp}\bar{\gamma}_Q}\right)^{m_{ss}} \tag{35}$$

Thus, utilizing (35) into (34), we have

$$F^{\infty}_{\bar{\gamma}_s X_{ss}}(x) = \left[\frac{\gamma\left(m_{sp}, \varepsilon_{sp}\bar{\gamma}_Q/\bar{\gamma}_t\right)}{\Gamma\left(m_{sp}\right)\Gamma\left(m_{ss}+1\right)}\left(\frac{\varepsilon_{ss}}{\bar{\gamma}_t}\right)^{m_{ss}} + \frac{\Gamma\left(m_{ss}+m_{sp}, \varepsilon_{sp}\bar{\gamma}_Q/\bar{\gamma}_t\right)}{\Gamma\left(m_{sp}\right)\Gamma\left(m_{ss}+1\right)}\left(\frac{\varepsilon_{ss}}{\varepsilon_{sp}\bar{\gamma}_Q}\right)^{m_{ss}}\right] x^{m_{ss}} \tag{36}$$

By substituting (36) into (7) in conjunction with [17, eq. (7.813.1)], the $F^{\infty}_{\gamma_d}(x)$ for the peak interference constraint can be calculated as

$$\begin{aligned} F^{\infty}_{\gamma_d}(x) = &\left[\frac{\gamma\left(m_{sp}, \varepsilon_{sp}\bar{\gamma}_Q/\bar{\gamma}_t\right)}{\Gamma\left(m_{sp}\right)\Gamma\left(m_{ss}+1\right)}\left(\frac{\varepsilon_{ss}}{\bar{\gamma}_t}\right)^{m_{ss}} + \frac{\Gamma\left(m_{ss}+m_{sp}, \varepsilon_{sp}\bar{\gamma}_Q/\bar{\gamma}_t\right)}{\Gamma\left(m_{sp}\right)\Gamma\left(m_{ss}+1\right)}\left(\frac{\varepsilon_{ss}}{\varepsilon_{sp}\bar{\gamma}_Q}\right)^{m_{ss}}\right] \\ &\times \frac{\alpha_{ps}\bar{\gamma}_p^k}{\Gamma\left(m_{ps}\right)\beta_{ps}^{k+1}}\sum_{k=0}^{m_{ss}}\binom{m_{ss}}{k}\mathrm{G}^{1,2}_{2,2}\left[-\delta_{ps}\middle|\begin{matrix}-k, 1-m_{ps}\\ 0, 0\end{matrix}\right] x^{m_{ss}} \end{aligned} \tag{37}$$

To this end, one can directly obtain the asymptotic OP by replacing x in (37) with γ_{th}.

REFERENCES

[1] B. Evans, M. Werner, E. Lutz, and *etal*, "Integration of satellite and terrestrial systems in funture media communications," *IEEE Trans. Wireless Commun.*, vol. 12, no. 5, pp. 72-80, Oct. 2005.

[2] G. Zheng, S. Chatzinotas, and B. Ottersten, "Generic optimization of linear precoding in multibeam satellite systems," *IEEE Trans. Wireless Commun.*, vol. 11, no. 6, pp. 2308-2320, Jun. 2012.

[3] A. Vanelli-Coralli, G. Corazza, and *etal*, "Satellite communications: Research trends and open issues," in *Proc. of the International Workshop on Satellite and Space Communications, IWSSC'07.*, 2007, pp. 71-75.

[4] S. Sreng, B. Escrig and M.-L. Boucheret, "Exact outage probability of a hybrid satellite terrestrial cooperative system with best relay selection," in *Proc. IEEE ICC 2013*,pp. 4520-4524, Budapest, Hungray, Jun. 2013.

[5] V. Sakarellos, C. Kourogiorgas and A. Panagopoulos, "Cooperative Hybrid Land Mobile Satellite-Terrestrial Broadcasting Systems: Outage Probability Evaluation and Accurate Simulation", *Wireless Personal Communications*, to be published.

[6] M. R. Bhatnagar and Arti M. K., "Performance analysis of AF based hybrid satellite-terrestrial cooperative network over generalized fading channels," *IEEE Commun. Lett.*, vol. 17, no. 10, pp. 1912-1915, Oct. 2013.

[7] K. An, M. Lin, J. Ouyang, Y. Huang and G. Zheng, "Symbol error analysis of hybrid satellite-terrestrial cooperative networks with co-channel interference" *IEEE Commun. Lett.*, vol. 18, no. 11, pp. 1947-1950, Nov. 2014.

[8] Arti M. K. and M. R. Bhatnagar, "Beamforming and combining in hybrid satellite-terrestrial cooperative systems," *IEEE Commun. Lett.*, vol. 18, no. 3, pp. 483-486, Mar. 2014.

[9] Goldsmith, S. A. Jafar, I. Maric, and S. Srinivasa, "Breaking spectrum gridlock with cognitive radios: an information theoretic perspective," *Proc. IEEE*, vol. 97, no. 5, pp. 894-914, May 2009.

[10] A. Ghasemi and E. S. Sousa, "Fundamental limits of spectrum-sharing in fading environments," *IEEE Trans. Wireless Commun.,*, vol. 6, no. 2, pp. 649-658, Feb. 2007.

[11] H. A. Suraweera, P. J. Smith, and M. Shafi, "Capacity limits and performance analysis of cognitive radio with imperfect channel knowledge," *IEEE Trans. Veh. Technol.*, vol. 59, no. 4, pp. 1811-1822, May 2010.

[12] S. Kandeepan, L. De Nardis, M.-G. Di Benedetto, A. Guidotti, and G. E. Corazza, "Cognitive satellite terrestrial radios," in *Proc. 2010 IEEE Global Telecommunications Conference*, pp. 1-6.

[13] S. K. Sharma, S. Chatzinotas, and B. Ottersten, "Satellite cognitive communications: interference modeling and techniques selection," in *Proc. 2012 ASMSC*, pp. 111-118.

[14] S. K. Sharma, S. Chatzinotas, and B. Ottersten , "Cognitive radio techniques for satellite communication systems," in *Proc. 2013 IEEE Vehicular Technology Conference*, pp. 1-5.

[15] S.Vassaki, M. I. Poulakis, A. D. Panagopoulos, and *etal*, "Power allocation in cognitive satellite terrestrial networks with QoS constraints", *IEEE Commun. Lett.*, vol. 17, no. 7, pp. 1344-1347, Jul. 2013.

[16] A. Abdi,W. Lau, M.-S. Alouini, and M. Kaveh, "A new simple model for land mobile satellite channels: first- and second-order statistics," *IEEE Trans. Wireless Commun.*, vol. 2, no. 3, pp. 519-528, May 2003.

[17] I. S. Gradshteyn and I. M. Ryzhik, *Table of Integrals, Series, and Products, 7th ed.* Academic Press, 2007.

[18] A. Papoulis, Probability, *Random Variables, and Stochastic Processes.* McGraw-Hill, 2002, 4th Ed

[19] R. P. Agrawal, "Certain transformation formulae and Meijer's G function of two variables," *Indian J. Pure Appl. Math.*, vol. 1, no. 4, 1970.

[20] S. Ansari, S. Al-Ahmadi, F. Yilmaz, and *etal*, "A new formula for the BER of binary modulations with dual-branch selection over generalized-K composite fading channels," *IEEE Trans. Commun.*, vol. 59, no. 10, pp. 2654-2658, Oct. 2011.

[21] V. S. Adamchik, O. I. Marichev, "The algorithm for calculating integrals of hypergeometric type functions and its realization in reduce systems," in *Proc. Int. Conf. Symp. Algebraic Comput.*, 1990, pp. 212-224.

[22] Z. Wang, and G. B. Giannakis, "A simple and general parameterization quantifying performance in fading channels,", *IEEE Trans. Commun.*, vol. 51, no. 8, pp. 1389-1398, Aug. 2003.

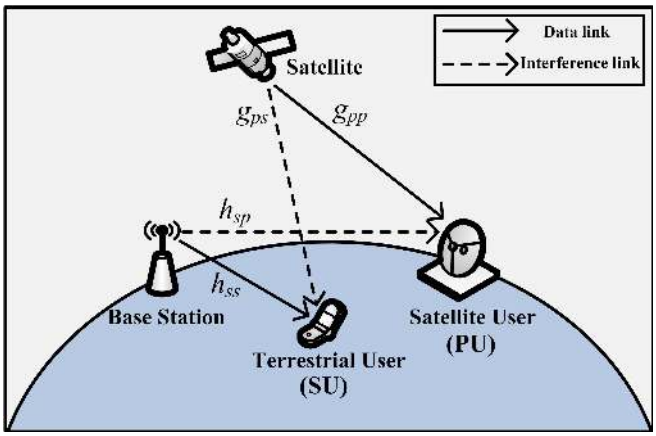

Fig. 1: System model of a cognitive hybrid satellite terrestrial network

TABLE I: LMS channel parameters [4]-[8]

Shadowing	b	m	Ω
Frequent heavy shadowing (FHS)	0.063	0.739	8.97×10^{-4}
Average shadowing (AS)	0.126	10.1	0.835
Infrequent light shadowing (ILS)	0.158	19.4	1.29

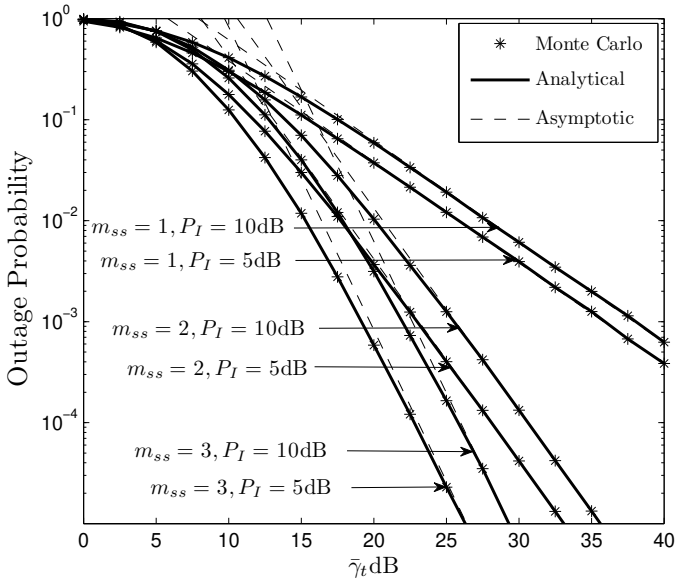

Fig. 2: Outage probability of the secondary network for different satellite interference powers under proportional interference constraint: h_{ps} experiencing FHS scenario, and $\bar{\gamma}_Q = \bar{\gamma}_t$

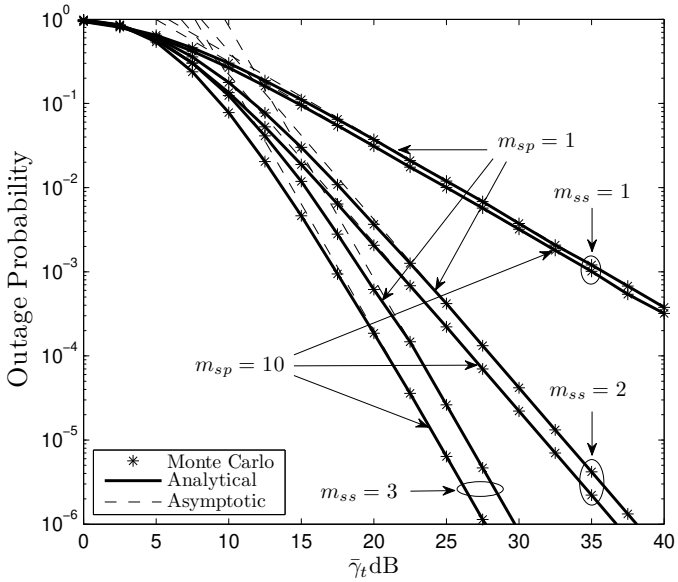

Fig. 3: Impact of fading severity of terrestrial interfering link (i.e., m_{sp}) on the outage probability of secondary network under proportional interference constraint: h_{ps} experiencing FHS, $P_p = 5$ dB and $\bar{\gamma}_Q = \bar{\gamma}_t$

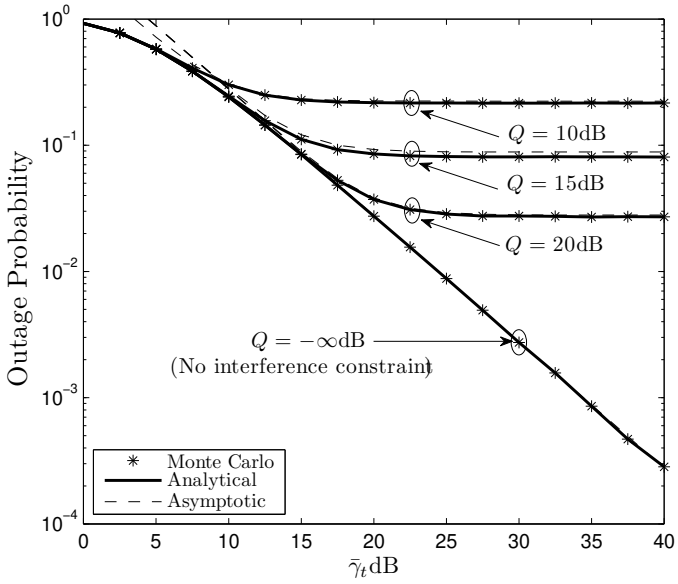

Fig. 4: Outage probability of the secondary network for different interference temperature constraints Q under peak interference constraint: h_{ps} experiencing FHS and $P_p = 5$ dB

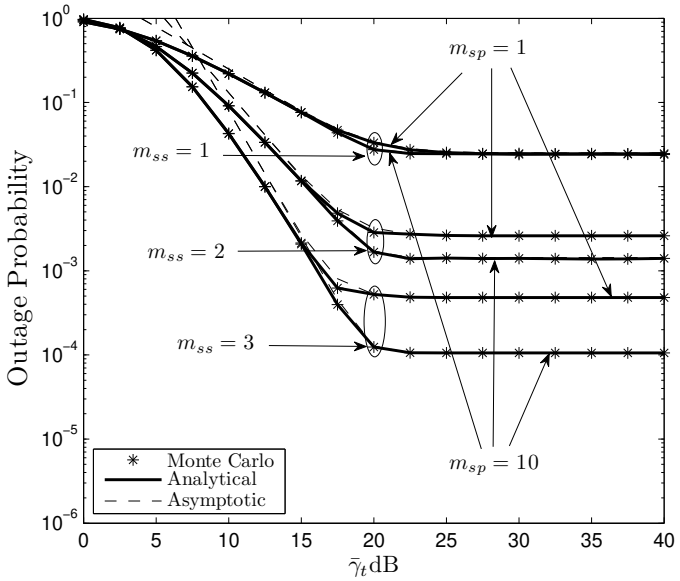

Fig. 5: Impact of fading severity of terrestrial interfering link (i.e., m_{sp}) on the outage probability of secondary network under peak interference constraint: h_{ps} experiencing FHS, $Q = 20$ dB and $P_p = 5$ dB

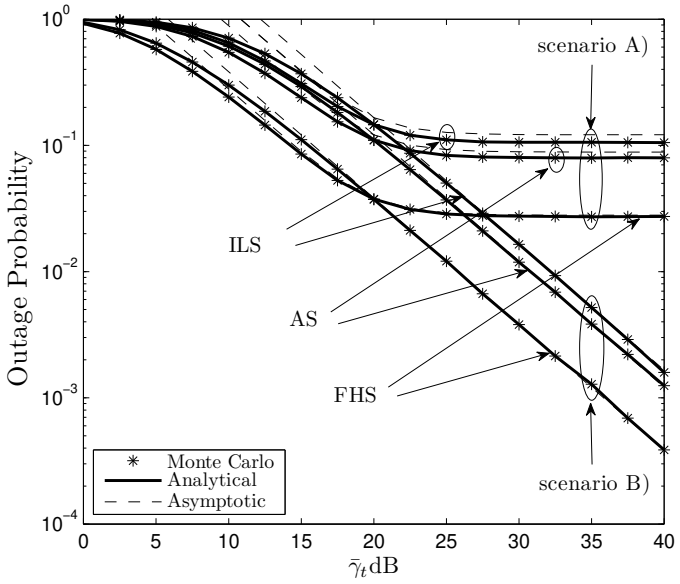

Fig. 6: Comparison between peak interference constraint and proportional interference constraint for different shadowing severity of satellite interfering link (i.e., $(b_{ps}, m_{ps}, \Omega_{ps})$): $m_{ss} = m_{sp} = 1$, $Q = 20$ dB, $P_p = 5$ dB and $\bar{\gamma}_Q = \bar{\gamma}_t$